

Truncated Gaussian basis approach for simulating many-body dynamics

Nico Albert,¹ Yueshui Zhang,² and Hong-Hao Tu^{2,1,*}

¹*Institut für Theoretische Physik, Technische Universität Dresden, 01062 Dresden, Germany*

²*Faculty of Physics and Arnold Sommerfeld Center for Theoretical Physics,
Ludwig-Maximilians-Universität München, 80333 Munich, Germany*

(Dated: October 8, 2024)

We propose a Truncated Gaussian Basis Approach (TGBA) for simulating the dynamics of quantum many-body systems. The approach constructs an effective Hamiltonian within a reduced subspace, spanned by fermionic Gaussian states, and diagonalizes it to obtain approximate eigenstates and eigenenergies. Symmetries can be exploited to perform parallel computation, enabling to simulate systems with much larger sizes. As an example, we compute the dynamic structure factor and study quench dynamics in a non-integrable quantum Ising chain, known as “ E_8 magnet”. The mass ratios calculated through the dynamic structure factor show excellent agreement with Zamolodchikov’s analytical predictions. For quench dynamics we observe that time-evolving wave functions in the truncated subspace facilitates the simulation of long-time dynamics.

Introduction — Efficient simulation of the dynamics of quantum many-body systems is an important yet challenging task in both experimental and theoretical physics [1–4]. It serves not only as a key method for exploring novel quantum phases and phase transitions in many-body physics, but also as a vital tool for investigating fundamental problems that bridge quantum and statistical physics, such as quantum chaos and thermalization [3]. However, computational methods are often hindered by the exponential growth of the Hilbert space dimension as the system size increases or the rapid entanglement growth as time evolves, leading to significant difficulties in simulating dynamics in quantum many-body systems [5–10].

The importance of simulating dynamics lies both in equilibrium and out of equilibrium scenarios. In equilibrium, real-frequency spectral functions contain crucial information about low-energy excitations and are directly linked to spectroscopic measurements. Due to the ill-conditioned nature of the analytic continuation [11–13] from the Matsubara frequency Green’s functions, it is desirable to compute spectral functions directly in real frequency [14–16]. For non-equilibrium dynamics, significant advancements have been made in studying quench problems in cold atom experiments [17–20]. However, as the initial state is typically far from the ground state, the entanglement entropy of time-evolved states often grows very rapidly with time (e.g., linear in time for one-dimensional critical systems [21]). This creates a substantial entanglement barrier, making it challenging to simulate long-time evolution in many-body systems with large sizes [22–25].

In this work, we introduce a new algorithm, the Truncated Gaussian Basis Approach (TGBA), for simulating the dynamics in quantum many-body systems. The algorithm reduces the full Hilbert space by keeping a subspace spanned by fermionic Gaussian states [26]. Within this subspace, fermionic Gaussian techniques enable us to diagonalize the truncated Hamiltonian and compute dy-

namical quantities, both in and out of equilibrium. Additionally, symmetries of the Hamiltonian, if available, can be fully exploited to perform parallel computations in different symmetry sectors. To demonstrate the power of our method, we apply it to the quantum Ising chain with both transverse and longitudinal fields. The dynamic structure factor is calculated and found to exhibit universal mass ratios which were predicted to emerge in the integrable E_8 Toda field theory [27]. These universal mass ratios have also been observed experimentally in certain quasi-one-dimensional materials [28–31]. We further demonstrate the capability of the TGBA to simulate non-equilibrium dynamics following a quantum quench. By calculating observables following a quench starting from a ferromagnetic initial state, we observe signatures of confinement between domain-wall excitations present after the quench [32]. These results indicate that the TGBA is a promising method in simulating many-body dynamics.

Method — In the TGBA, our main targets are Hamiltonians of the form $H = H_0 + V$, where H_0 , the “free part”, is (or can be mapped to) a fermionic quadratic Hamiltonian [33] so that one has full information about its spectrum $\{E_\alpha^{(0)}\}$ and eigenstates $|\phi_\alpha\rangle \in \mathcal{H}$ (\mathcal{H} : full Hilbert space). The eigenstates $|\phi_\alpha\rangle$ are (pure) fermionic Gaussian states [34]. Restricting to a suitable subspace $\mathcal{H}_{\text{trunc}} \subset \mathcal{H}$, a variational ansatz for the eigenstates of the full Hamiltonian H can be constructed from the eigenstates of H_0 :

$$|\psi_\alpha\rangle = \sum_{|\phi_\beta\rangle \in \mathcal{H}_{\text{trunc}}} M_{\alpha\beta} |\phi_\beta\rangle. \quad (1)$$

The optimal superposition coefficients $\{M_{\alpha\beta}\}$ and the approximated eigenenergies $\{E_\alpha\}$ of the full Hamiltonian are determined by diagonalizing the effective Hamiltonian in the truncated subspace:

$$H_{\alpha\beta} \equiv \langle \phi_\alpha | H | \phi_\beta \rangle = E_\alpha^{(0)} \delta_{\alpha\beta} + \langle \phi_\alpha | V | \phi_\beta \rangle \quad (2)$$

with $|\phi_\alpha\rangle \in \mathcal{H}_{\text{trunc}}$. If no truncation were performed, the method would be exact. However, in practice, one can only keep a maximum of χ states in $\mathcal{H}_{\text{trunc}}$ and work with a χ -dimensional *truncated* Hamiltonian. The quality of this approximation depends not only on the truncation dimension χ , but also on the truncation criterion, which we will comment on later. The errors incurred by the truncation can be quantified by comparing the TGBA data (e.g., physical observables) with successively increasing χ .

If the Hamiltonian H has a symmetry which is shared by H_0 and V , it can be fully exploited in the TGBA. The truncated Hilbert space has a block structure, $\mathcal{H}_{\text{trunc}} = \oplus_a \mathcal{H}_{a,\text{trunc}}$, where a labels different symmetry sectors. Using the fermionic Gaussian eigenbasis of H_0 , $|\phi_{a,\alpha}\rangle \in \mathcal{H}_{a,\text{trunc}}$, a truncated Hamiltonian is defined in each sector, $H_{(a,\alpha);(a,\beta)} = \langle \phi_{a,\alpha} | H | \phi_{a,\beta} \rangle$, which can be diagonalized independently. This allows one to carry out parallel computation and simulate much larger system sizes which would be impossible otherwise. In the Ising chain example below, we will illustrate how to make use of translation symmetry in the TGBA.

The truncation criterion determines whether the TGBA will succeed or not. For most applications in equilibrium (e.g., determining the spectrum of H or calculating dynamic correlation functions), a natural way to perform the truncation is to retain χ lowest energy states of H_0 in $\mathcal{H}_{\text{trunc}}$. This is of the same spirit as Wilson's NRG [35] and the truncated conformal space approach [36–42], which can be justified when the V term is weak in some sense. However, for certain applications, different truncation schemes might be more suited to construct $\mathcal{H}_{\text{trunc}}$. For instance, when simulating quench dynamics, we observe that retaining those states which have largest overlaps with the initial state is a more appropriate metric.

Example — To illustrate how the TGBA works, we choose the quantum Ising chain with both transverse and longitudinal fields as a paradigmatic example:

$$\begin{aligned} H_0 &= - \sum_{j=1}^N \sigma_j^x \sigma_{j+1}^x - h_\perp \sum_{j=1}^N \sigma_j^z, \\ V &= -h_\parallel \sum_{j=1}^N \sigma_j^x, \end{aligned} \quad (3)$$

where σ_j^α ($\alpha = x, y, z$) are Pauli operators at site j and N is the total number of sites. We consider $h_\perp > 0$ and even N throughout this work and impose periodic boundary conditions ($\sigma_{N+1}^\alpha = \sigma_1^\alpha$) to preserve translation symmetry.

As the “free part” of the full Hamiltonian, H_0 corresponds to the transverse-field Ising chain [43], which, using the Jordan-Wigner transformation $\sigma_j^x = (c_j + c_j^\dagger)(-1)^{\sum_{i=1}^{j-1} c_i^\dagger c_i}$ and $\sigma_j^z = 2c_j^\dagger c_j - 1$, is mapped to a

fermionic Hamiltonian:

$$\begin{aligned} H_0 &= \sum_{j=1}^{N-1} (c_j - c_j^\dagger)(c_{j+1} + c_{j+1}^\dagger) - Q(c_N - c_N^\dagger)(c_1 + c_1^\dagger) \\ &\quad - h_\perp \sum_{j=1}^N (2c_j^\dagger c_j - 1). \end{aligned} \quad (4)$$

The fermion parity operator $Q = (-1)^{\sum_{j=1}^N c_j^\dagger c_j}$ commutes with H_0 and has eigenvalues ± 1 . Thus, the eigenstates of H_0 fall into two sectors: the Neveu-Schwarz (NS) sector with $Q = 1$, and the Ramond (R) sector with $Q = -1$. In the NS (R) sector, H_0 in Eq. (4) becomes quadratic, and one may impose anti-periodic (periodic) boundary condition $c_{N+1} = -c_1$ ($c_{N+1} = c_1$) for the Jordan-Wigner fermions. After performing the Fourier transformation $c_j = \frac{1}{\sqrt{N}} \sum_{q \in \text{NS/R}} e^{iqj} c_q$ and a Bogouliubov transformation, H_0 is diagonalized as

$$H_0^{\text{NS/R}} = \sum_{q \in \text{NS/R}} \varepsilon_q \left(d_q^\dagger d_q - \frac{1}{2} \right) \quad (5)$$

with

$$\varepsilon_q = \begin{cases} 2\sqrt{(h_\perp - 1)^2 + 4h_\perp \cos^2(q/2)} & q \neq \pi \\ 2(h_\perp - 1) & q = \pi \end{cases}, \quad (6)$$

where allowed single-particle momenta in the NS and R sector are $q = \pm \frac{\pi}{N}, \pm \frac{3\pi}{N}, \dots, \pm \frac{(N-1)\pi}{N}$ and $q = 0, \pm \frac{2\pi}{N}, \dots, \pm \frac{(N-2)\pi}{N}, \pi$, respectively. The Bogouliubov mode in Eq. (5) is given by $d_q = \sin(\theta_q/2)c_q - i \cos(\theta_q/2)c_{-q}^\dagger$ with $\theta_q = \text{sign}(q) \arccos \frac{2(h_\perp + \cos q)}{\varepsilon_q} \in (-\pi, \pi]$. The ground states in the NS- and the R-sector read $|0\rangle_{\text{NS/R}} = [\prod_{0 < q \in \text{NS/R}} \cos(\theta_q/2)]^{-1} \prod_{q \in \text{NS/R}, q \neq \pi} d_q |0\rangle_c$, where $|0\rangle_c$ is the vacuum of Jordan-Wigner fermions. Thus, all eigenstates of H_0 are written as $d_{q_1}^\dagger d_{q_2}^\dagger \dots d_{q_M}^\dagger |0\rangle_{\text{NS/R}}$ (M even), with distinct single-particle momenta $q_1 < q_2 < \dots < q_M$ in the respective sector. They form the full Hilbert space $\mathcal{H} = \oplus_k \mathcal{H}_k$, where the many-body momentum of eigenstates, $k = \sum_{j=1}^M q_j \pmod{2\pi}$, labels different symmetry sectors.

To set up the TGBA, we define the truncated subspace as $\mathcal{H}_{\text{trunc}} = \oplus_k \mathcal{H}_{k,\text{trunc}}$, with basis vectors $\{|\phi_{k,\alpha}\rangle\}$ ($\alpha = 1, \dots, \chi$) [44]. The retained basis vectors are selected from the eigenstates of H_0 described above, according to which selection criterion depends on the specific application. A crucial technical step in the TGBA is to compute the matrix elements of the V term [Eq. (3)] in the truncated subspace. As the V term is translation-invariant, it does not mix basis vectors with different momenta. Within the $\mathcal{H}_{k,\text{trunc}}$ subspace, matrix elements of V read $\langle \phi_{k,\alpha} | V | \phi_{k,\beta} \rangle = -Nh_\parallel \langle \phi_{k,\alpha} | (c_1^\dagger + c_1) | \phi_{k,\beta} \rangle$. Using Wick's theorem [45], evaluating such matrix elements reduces to computing the Pfaffian of a matrix [46–49] with

dimension of at most $\mathcal{O}(N^2)$, which can be calculated efficiently for system sizes up to $N \sim 100$ [50].

Dynamic structure factor — We first demonstrate the computation of the longitudinal dynamical structure factor

$$S^{xx}(k, \omega) = \frac{1}{N} \sum_{j,l=1}^N e^{-ik(j-l)} \int_{-\infty}^{\infty} dt e^{i\omega t} \langle \sigma_j^x(t) \sigma_l^x(0) \rangle \quad (7)$$

for the Ising chain (3) at zero temperature. For this calculation, we adopt $h_{\perp} = 1$ and $h_{\parallel} = 0.05$ with chain length $N = 60$. The model can hence be viewed as a critical Ising chain perturbed by a longitudinal field, whose low-energy effective theory is the integrable E_8 Toda field theory exhibiting eight massive excitations (“particles”) with universal mass ratios [27].

For computing the dynamic structure factor, we retain $\chi = 1600$ lowest energy eigenstates of H_0 in each momentum sector and diagonalize the effective Hamiltonians to obtain (approximate) eigenstates $|\psi_{k,\alpha}\rangle = \sum_{\beta=1}^{\chi} [M(k)]_{\alpha\beta} |\phi_{k,\beta}\rangle$ as well as their corresponding variational energies with respect to the full Hamiltonian H . The ground state lies in the $k = 0$ sector, which is denoted as $|\psi_{0,1}\rangle$ (with energy $E_{0,1}$). Inserting the approximated time evolution operator $e^{-iHt} \simeq \sum_k \sum_{\alpha=1}^{\chi} e^{-iE_{k,\alpha}t} |\psi_{k,\alpha}\rangle \langle \psi_{k,\alpha}|$ into Eq. (7), the dynamical structure factor becomes

$$S^{xx}(k, \omega) \simeq 2\pi \sum_{\alpha=1}^{\chi} |\langle \psi_{0,1} | \sigma_k^x | \psi_{k,\alpha} \rangle|^2 \delta(\omega + E_{0,1} - E_{k,\alpha}) \quad (8)$$

with $\sigma_k^x = \frac{1}{\sqrt{N}} \sum_{j=1}^N e^{-ikj} \sigma_j^x$. Using translation symmetry, the matrix elements in Eq. (8) become $\langle \psi_{0,1} | \sigma_k^x | \psi_{k,\alpha} \rangle = \sqrt{N} e^{-ik} \sum_{\mu,\nu=1}^{\chi} [M(0)]_{1,\mu}^* \langle \phi_{0,\mu} | (c_1^\dagger + c_1) | \phi_{k,\nu} \rangle [M(k)]_{\alpha,\nu}$, which also reduce to Pfaffian computations [45].

The numerically computed $S^{xx}(k, \omega)$ is depicted in Fig. 1(a). It provides spectral information beyond the low-energy limit (with full momentum resolution) and is readily comparable to experiments. The E_8 Toda field theory predicts eight massive particles [27, 51], whose masses are universal up to a mass scale set by $m_1 \sim h_{\parallel}^{8/15}$ [52]. Seven out of the eight massive particles can be reliably identified in our calculated $S^{xx}(k=0, \omega)$, as shown in Fig. 1(b). The retained $\chi = 1600$ states in $k = 0$ sector corresponds to a cutoff energy at $E_{\text{cut}} \simeq 5.4 \simeq 4.9 m_1$. The mass of the heaviest particle, with theoretical value $m_8 \simeq 4.78 m_1$ [27], is too close to E_{cut} and has not converged properly in our $\chi = 1600$ calculation. For comparison, the numerical values of six mass ratios from the TGBA calculation and the values predicted by the E_8 Toda field theory are displayed in Table I.

Quench dynamics — We now employ the TGBA to simulate dynamics following a quantum quench. Hamil-

	m_2/m_1	m_3/m_1	m_4/m_1	m_5/m_1	m_6/m_1	m_7/m_1
TGBA	1.616	1.982	2.401	2.959	3.260	3.887
E_8 theory	1.618	1.989	2.405	2.956	3.218	3.891

TABLE I. Peak ratios of the E_8 single-particle states obtained from the TGBA calculation versus the analytical prediction from the E_8 Toda field theory [27].

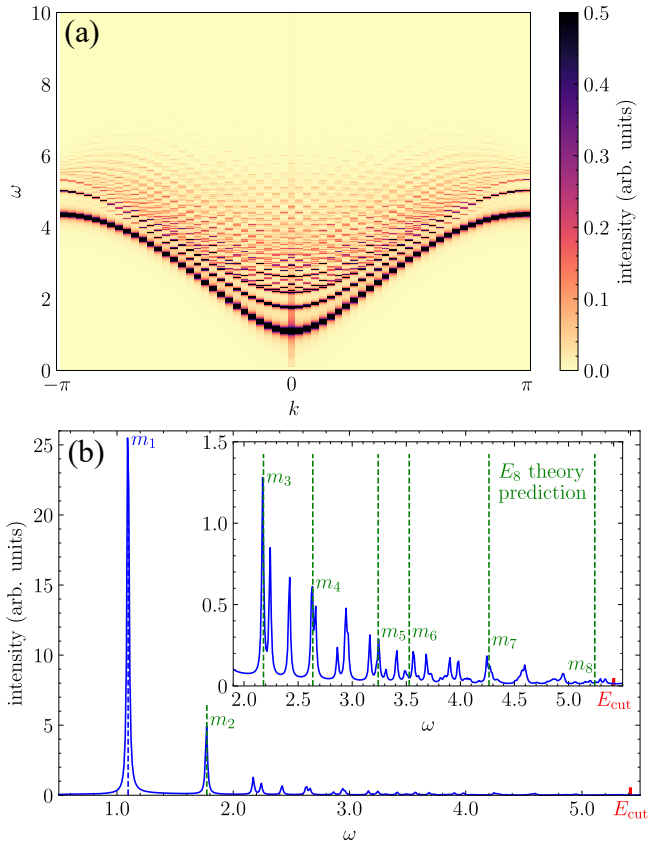


FIG. 1. (a) Dynamic structure factor $S^{xx}(k, \omega)$ at $h_{\perp} = 1$ and $h_{\parallel} = 0.05$ for a chain of $N = 60$ sites. (b) Dynamic structure factor $S^{xx}(k = 0, \omega)$. The dashed lines represent the analytical predictions of the E_8 masses. The lowest energy $E_{0,1}$ has been shifted to zero.

tonian truncation methods have already been used to simulate quench dynamics in the Ising field theory, using either the Ising conformal field theory or the massive Majorana field theory to construct the basis of the truncated subspace [53–55]. The method we employ here is of a similar spirit, however we find that choosing a different truncation scheme can improve the performance of the TGBA significantly.

Quantum quenches are the simplest type of non-equilibrium dynamics. The system is prepared in some initial state $|\Phi_0\rangle$, which we choose to be an eigenstate of the transverse-field Ising chain $H_0(t=0)$. Then both the transverse and longitudinal fields are quenched. To perform the simulation, we decompose the Hamiltonian after the quench again into a “free” and an interact-

ing part, $H(t > 0) = H_0(t > 0) + V(t > 0)$, and approximate the time evolution operator $e^{-iH(t>0)t} \simeq \sum_{\alpha=1}^{\chi} e^{-iE_{\alpha}t} |\psi_{\alpha}\rangle\langle\psi_{\alpha}|$ within the TGBA using the eigenbasis of $H_0(t > 0)$. Denoting this eigenbasis again by $\{|\phi_{\alpha}\rangle\}$, the time evolution of the initial state is then given by

$$e^{-iH(t>0)t}|\Phi_0\rangle \simeq \sum_{\alpha=1}^{\chi} B_{\alpha}(t)|\phi_{\alpha}\rangle \quad (9)$$

with $B_{\alpha}(t) = \sum_{\alpha=1}^{\chi} e^{-iE_{\alpha}t} \langle\psi_{\alpha}|\Phi_0\rangle$. The coefficients $B_{\alpha}(t)$ contain approximate eigenenergies and the ansatz for the eigenstates obtained from the TGBA, as well as overlaps of the initial state with states from the truncated subspace $\langle\phi_{\alpha}|\Phi_0\rangle$. To fully capture the dynamics of the time-evolved state it is not only necessary to obtain a good approximation for the spectrum and eigenstates of $H(t > 0)$, it also must be made sure that the truncated subspace sufficiently captures the initial state $|\Phi_0\rangle$. For the cases considered below, where the perturbation $V(t > 0)$ is weak, we find that capturing $|\Phi_0\rangle$ is substantially more challenging than approximating the spectrum and eigenstates. To overcome this we construct the truncated subspace by ordering states by their overlap with $|\Phi_0\rangle$ instead of their bare energies $E_{\alpha}^{(0)}$, we find that this reduces the number of states that need to be included in $\mathcal{H}_{\text{trunc}}$ drastically. How well the initial state is captured by the truncated subspace can be easily checked by calculating $\sum_{\alpha=1}^{\chi} |\langle\phi_{\alpha}|\Phi_0\rangle|^2 \leq \langle\Phi_0|\Phi_0\rangle = 1$. Also note that the TGBA approximation for the time-evolved state is not exactly normalized, but its norm is time-independent and coincides with the overlap of the truncated subspace with the initial state: $\|e^{-iH(t>0)t}|\Phi_0\rangle\| \simeq \sqrt{\sum_{\alpha=1}^{\chi} |\langle\phi_{\alpha}|\Phi_0\rangle|^2}$. Remarkably, we find, at least in the case of small h_{\parallel} we consider here, that the TGBA remains converged up to very long times once the initial state is sufficiently captured within the truncated subspace.

To obtain a quantitative measure for convergence of the TGBA data, independent of what observables we consider, we calculate the norm of the difference of two successive TGBA approximations with different truncation dimensions. This quantity will be time-dependent, to define a metric between the approximations we take the maximum of this difference over some time span $[0, t_{\text{max}}]$. In terms of the coefficients $B_{\alpha}(t)$, this metric can be expressed as

$$\begin{aligned} \varepsilon(\chi', \chi) &= \max_{t \in [0, t_{\text{max}}]} \left\| |\Psi^{\chi}(t)\rangle - |\Psi^{\chi'}(t)\rangle \right\| \\ &= \max_{t \in [0, t_{\text{max}}]} \sqrt{\sum_{\alpha=1}^{\chi} |B_{\alpha}^{\chi}(t) - B_{\alpha}^{\chi'}(t)|^2 + \sum_{\alpha=\chi+1}^{\chi'} |B_{\alpha}^{\chi'}(t)|^2}, \end{aligned} \quad (10)$$

where $|\Psi^{\chi}(t)\rangle$ and $|\Psi^{\chi'}(t)\rangle$ denote two approximations of the time-evolved state with truncation dimension χ and χ' ($\chi < \chi'$), respectively. $B_{\alpha}^{\chi}(t)$ and $B_{\alpha}^{\chi'}(t)$ are the corresponding coefficients in the respective truncated subspaces.

To probe the method, we calculate the time evolution of the longitudinal magnetization $\langle\sigma^x\rangle(t)$ subject to the following quench protocol: the system is initialized in the ferromagnetic ground state of the transverse-field Ising chain with $\langle\sigma^x\rangle > 0$, for some $h_{\perp}(t=0) < 1$. Since this state has many-body momentum $k=0$, only states in the $k=0$ sector need to be included in the truncated subspace, which greatly reduces the computational cost. Then we quench the Hamiltonian to the E_8 region, i.e., we apply a Hamiltonian with a critical transverse field $h_{\perp}(t > 0) = 1$ and a small longitudinal field $h_{\parallel}(t > 0) > 0$. The longitudinal field induces confinement between the excitations (domain walls) emerging from the ferromagnetic initial state after the quench, leading to a characteristic oscillatory behaviour in the longitudinal magnetization [32]. For $h_{\perp}(t > 0) = 1$ the excitations in the scaling limit can be described by the E_8 theory, and the E_8 masses and gaps between them appear as peaks in the power spectrum of the magnetization $|\langle\sigma^x\rangle(\omega)|^2$.

Figure 2 depicts the results from the TGBA calculation for a quench $(h_{\perp}, h_{\parallel}) = (0.5, 0) \mapsto (1.0, 0.05)$ for different truncation dimensions, as well as the corresponding power spectrum. To judge the quality of the TGBA approximation, we calculate the metric $\varepsilon(\chi', \chi)$ for successive approximations as well. For the power spectrum the E_8 masses as well as gaps between them serve as additional benchmarks. Peaks that are unlabelled correspond to multi-particle states where the individual particles carry non-vanishing single-particle momenta.

We restrict ourselves to this specific quench protocol so that we can use analytical results from the E_8 theory as additional benchmarks, however since we are working with a lattice model, we are by no means restricted to a critical $H_0(t > 0)$ after the quench.

Summary and outlook — To summarize, we have proposed a new method, the TGBA, to simulate dynamics of quantum many-body systems. A key feature of the TGBA is that the effective Hamiltonian can be efficiently constructed and simulated within the truncated Gaussian subspace, both in and out of equilibrium. The non-integrable quantum Ising chain example demonstrates that, using appropriate truncation schemes, (i) the calculated dynamic structure factor accurately reproduces the universal mass ratios and provides the spectral information beyond the low-energy limit; (ii) the calculated physical observables following a quantum quench can be efficiently simulated in long times. It will be interesting to apply the TGBA to other interesting systems, such as Hubbard-type models.

For the simulations we considered in this work, con-

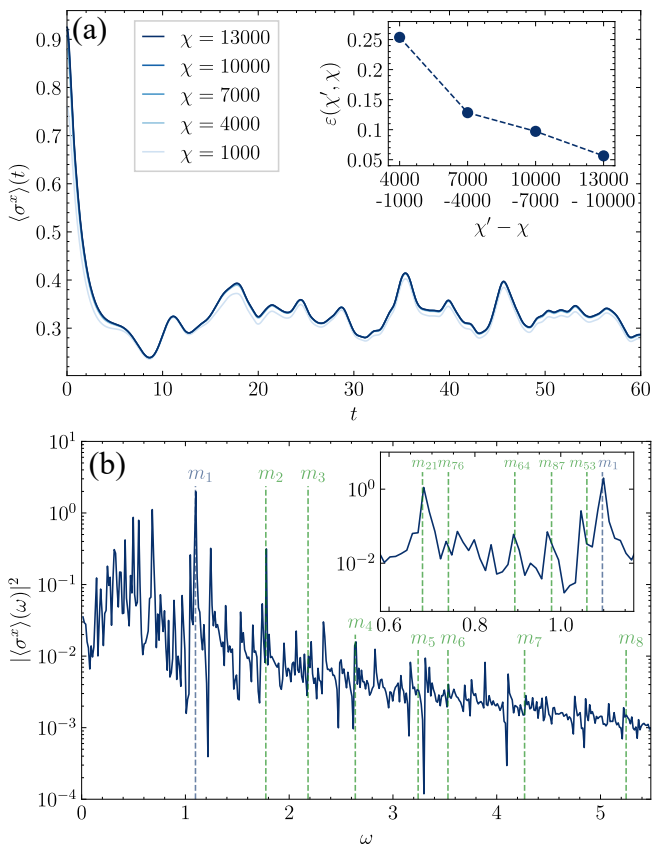


FIG. 2. Longitudinal magnetization following a global quench $(h_{\perp}, h_{\parallel}) = (0.5, 0) \mapsto (1.0, 0.05)$ from the initial state $|\Phi_0\rangle$ with positive magnetization, for a chain of $N = 60$ sites. (a) Time evolution of the longitudinal magnetization $\langle \sigma^x \rangle(t)$ up to $t_{\max} = 60$. Inset: metric ε between successive approximations, as defined in Eq. (10). (b) Power spectrum $|\langle \sigma^x \rangle(\omega)|^2$. The Fourier transform was performed for times up to $t = 480$. The E_8 masses as well as gaps between them, denoted by $m_{ij} = m_i - m_j$, are marked in green. Unlabelled peaks correspond to multi-particle states that carry non-vanishing one-particle momenta.

vergence is typically achieved for truncation dimensions of order $\chi \sim 1000 - 10000$ (in each momentum sector), a range where the computational cost of diagonalizing the effective Hamiltonian is still quite small. For more challenging problems it is possible to improve the TGBA by adopting the idea of NRG [35, 56] or DMRG [57] and constructing the retained subspace iteratively, which may further improve the accuracy of the method.

Acknowledgments — We are grateful to Mari Carmen Bañuls, Jan Carl Budich, Jan von Delft, Andreas Gleis, Michael Knap, Oleksandra Kovalska, Goran Nakerst, Frank Pollmann, Wei Tang, Lei Wang, and Tao Xiang for helpful discussions. N.A. is supported by the Deutsche Forschungsgemeinschaft (DFG) through project A06 of SFB 1143 (Project No. 247310070). Y.S.Z. is supported by the Sino-German (CSC-DAAD) Postdoc Scholarship Program. The authors gratefully acknowledge the

computing time made available to them on the high-performance computer at the NHR Center of TU Dresden. This center is jointly supported by the Federal Ministry of Education and Research and the state governments participating in the NHR [58].

* h.tu@lmu.de

- [1] A. Polkovnikov, K. Sengupta, A. Silva, and M. Vengalattore, *Rev. Mod. Phys.* **83**, 863 (2011).
- [2] I. M. Georgescu, S. Ashhab, and F. Nori, *Rev. Mod. Phys.* **86**, 153 (2014).
- [3] L. D'Alessio, Y. Kafri, A. Polkovnikov, and M. Rigol, *Adv. Phys.* **65**, 239–362 (2016).
- [4] D. A. Abanin, E. Altman, I. Bloch, and M. Serbyn, *Rev. Mod. Phys.* **91**, 021001 (2019).
- [5] G. Vidal, *Phys. Rev. Lett.* **91**, 147902 (2003).
- [6] S. R. White and A. E. Feiguin, *Phys. Rev. Lett.* **93**, 076401 (2004).
- [7] A. J. Daley, C. Kollath, U. Schollwöck, and G. Vidal, *J. Stat. Mech.: Theory Exp.* **2004**, P04005 (2004).
- [8] J. Haegeman, J. I. Cirac, T. J. Osborne, I. Pižorn, H. Verschelde, and F. Verstraete, *Phys. Rev. Lett.* **107**, 070601 (2011).
- [9] J. Haegeman, C. Lubich, I. Oseledets, B. Vandereycken, and F. Verstraete, *Phys. Rev. B* **94**, 165116 (2016).
- [10] J.-W. Li, A. Gleis, and J. von Delft, *Phys. Rev. Lett.* **133**, 026401 (2024).
- [11] M. Jarrell and J. Gubernatis, *Phys. Rep.* **269**, 133 (1996).
- [12] A. W. Sandvik, *Phys. Rev. B* **57**, 10287 (1998).
- [13] J. Fei, C.-N. Yeh, and E. Gull, *Phys. Rev. Lett.* **126** (2021).
- [14] S. R. White and I. Affleck, *Phys. Rev. B* **77**, 134437 (2008).
- [15] A. Holzner, A. Weichselbaum, I. P. McCulloch, U. Schollwöck, and J. von Delft, *Phys. Rev. B* **83**, 195115 (2011).
- [16] A. Nocera and G. Alvarez, *Phys. Rev. E* **94**, 053308 (2016).
- [17] M. Cheneau, P. Barmettler, D. Poletti, M. Endres, P. Schauß, T. Fukuhara, C. Gross, I. Bloch, C. Kollath, and S. Kuhr, *Nature* **481**, 484 (2012).
- [18] F. Meinert, M. J. Mark, E. Kirilov, K. Lauber, P. Weinmann, A. J. Daley, and H.-C. Nägerl, *Phys. Rev. Lett.* **111**, 053003 (2013).
- [19] T. Langen, R. Geiger, M. Kuhnert, B. Rauer, and J. Schmiedmayer, *Nat. Phys.* **9**, 640 (2013).
- [20] A. M. Kaufman, M. E. Tai, A. Lukin, M. Rispoli, R. Schittko, P. M. Preiss, and M. Greiner, *Science* **353**, 794 (2016).
- [21] P. Calabrese and J. Cardy, *J. Stat. Mech.: Theory Exp.* **2005**, P04010 (2005).
- [22] M. C. Bañuls, M. B. Hastings, F. Verstraete, and J. I. Cirac, *Phys. Rev. Lett.* **102**, 240603 (2009).
- [23] A. Müller-Hermes, J. I. Cirac, and M. C. Bañuls, *New J. Phys.* **14**, 075003 (2012).
- [24] M. Frías-Pérez and M. C. Bañuls, *Phys. Rev. B* **106**, 115117 (2022).
- [25] C. Lamb, Y. Tang, R. Davis, and A. Roy, *Nat. Commun.* **15**, 5901 (2024).
- [26] The pure fermionic Gaussian states are also known as

- Hartree-Fock-Bogoliubov states. In the absence of pairing, they reduce to Hartree-Fock states.
- [27] A. B. Zamolodchikov, *Int. J. Mod. Phys. A* **4**, 4235 (1989).
- [28] R. Coldea, D. A. Tennant, E. M. Wheeler, E. Wawrzynska, D. Prabhakaran, M. Telling, K. Habicht, P. Smeibidl, and K. Kiefer, *Science* **327**, 177 (2010).
- [29] K. Amelin, J. Engelmayer, J. Viirok, U. Nagel, T. Rõ om, T. Lorenz, and Z. Wang, *Phys. Rev. B* **102**, 104431 (2020).
- [30] Z. Zhang, K. Amelin, X. Wang, H. Zou, J. Yang, U. Nagel, T. Rõ om, T. Dey, A. A. Nugroho, T. Lorenz, J. Wu, and Z. Wang, *Phys. Rev. B* **101**, 220411 (2020).
- [31] H. Zou, Y. Cui, X. Wang, Z. Zhang, J. Yang, G. Xu, A. Okutani, M. Hagiwara, M. Matsuda, G. Wang, G. Mussardo, K. Hódsági, M. Kormos, Z. He, S. Kimura, R. Yu, W. Yu, J. Ma, and J. Wu, *Phys. Rev. Lett.* **127**, 077201 (2021).
- [32] M. Kormos, M. Collura, G. Takács, and P. Calabrese, *Nat. Phys.* **13**, 246 (2017).
- [33] While H_0 is often part of H , one may also take H_0 as a “mean-field” approximation of H and $V = H - H_0$.
- [34] S. Bravyi, *Quantum Inf. and Comp.* **5**, 216 (2005).
- [35] K. G. Wilson, *Rev. Mod. Phys.* **47**, 773 (1975).
- [36] V. P. Yurov and A. B. Zamolodchikov, *Int. J. Mod. Phys. A* **5**, 3221 (1990).
- [37] V. P. Yurov and A. B. Zamolodchikov, *Int. J. Mod. Phys. A* **6**, 4557 (1991).
- [38] M. Lässig, G. Mussardo, and J. L. Cardy, *Nucl. Phys. B* **348**, 591 (1991).
- [39] M. Beria, G. Brandino, L. Lepori, R. Konik, and G. Sierra, *Nucl. Phys. B* **877**, 457 (2013).
- [40] R. Konik, T. Pálmai, G. Takács, and A. Tsvelik, *Nucl. Phys. B* **899**, 547 (2015).
- [41] A. J. A. James, R. M. Konik, P. Lecheminant, N. J. Robinson, and A. M. Tsvelik, *Rep. Prog. Phys.* **81**, 046002 (2018).
- [42] G. Mussardo, *Statistical Field Theory: An Introduction to Exactly Solved Models in Statistical Physics* (Oxford University Press, Oxford, 2020).
- [43] P. Pfeuty, *Ann. Phys.* **57**, 79 (1970).
- [44] For simplicity, we use the same truncation dimension χ across all momentum sectors.
- [45] See the Appendix for further technical details.
- [46] G. F. Bertsch and L. M. Robledo, *Phys. Rev. Lett.* **108**, 042505 (2012).
- [47] B. G. Carlsson and J. Rotureau, *Phys. Rev. Lett.* **126**, 172501 (2021).
- [48] H.-K. Jin, R.-Y. Sun, Y. Zhou, and H.-H. Tu, *Phys. Rev. B* **105**, L081101 (2022).
- [49] E. Mascot, T. Hodge, D. Crawford, J. Bedow, D. K. Morr, and S. Rachel, *Phys. Rev. Lett.* **131**, 176601 (2023).
- [50] M. Wimmer, *ACM Trans. Math. Softw.* **38**, 1 (2012).
- [51] J. A. Kjäll, F. Pollmann, and J. E. Moore, *Phys. Rev. B* **83**, 020407 (2011).
- [52] To ensure the results are not dominated by finite-size effects, the correlation length $\xi \sim m_1^{-1} \sim h_{\parallel}^{-8/15}$ should be small compared to the length of the chain. We find that for $h_{\parallel} = 0.05$ this is still the case.
- [53] T. Rakovszky, M. Mestyán, M. Collura, M. Kormos, and G. Takács, *Nucl. Phys. B* **911**, 805 (2016).
- [54] I. Kukuljan, S. Sotiriadis, and G. Takacs, *Phys. Rev. Lett.* **121**, 110402 (2018).
- [55] K. Hódsági, M. Kormos, and G. Takács, *SciPost Phys.* **5**, 027 (2018).
- [56] R. M. Konik and Y. Adamov, *Phys. Rev. Lett.* **98**, 147205 (2007).
- [57] S. R. White, *Phys. Rev. Lett.* **69**, 2863 (1992).
- [58] www.nhr-verein.de/unsere-partner.

APPENDIX

Pfaffian formula for matrix elements

Setting up the effective Hamiltonian in the truncated subspace spanned by fermionic Gaussian states requires an efficient method to calculate the matrix elements of operators in the kept subspace. This can be achieved using Wick's theorem. Let us consider N fermionic modes, with creation (annihilation) operators c_j^\dagger (c_j). Denote the vacuum of the fermionic modes by $|0\rangle_c$, with $c_j|0\rangle_c = 0 \forall j$. Now, consider a product of $2n$ operators \mathcal{O}_m that can be written as a linear combination of the fermionic modes: $\mathcal{O}_m = \sum_{j=1}^N (U_{jm}c_j^\dagger + V_{jm}c_j)$. The expectation value of these operators in the c -vacuum can then be written as the Pfaffian of a $2n \times 2n$ matrix A ,

$${}_c\langle 0 | \mathcal{O}_1 \dots \mathcal{O}_{2n} | 0 \rangle_c = \text{Pf}(A), \quad (\text{S1})$$

where A is skew-symmetric, and its upper triangular part is given by the upper triangular (u.t.) part $(V^T U)|_{\text{u.t.}}$ of $V^T U$:

$$A = \begin{pmatrix} 0 & & & (V^T U)|_{\text{u.t.}} \\ & \ddots & & \\ & & \ddots & \\ -[(V^T U)|_{\text{u.t.}}]^T & & & 0 \end{pmatrix}. \quad (\text{S2})$$

In both the NS- and the R-sector, eigenstates of the transverse-field Ising chain are given by an even number of Bogoliubov modes $d_q^\dagger = \sin(\theta_q/2)c_q^\dagger + i \cos(\theta_q/2)c_{-q}$ applied to some fermionic Gaussian vacuum state $|0\rangle_{\text{NS/R}}$, where $\theta_q = \text{sign}(q) \arccos\left(\frac{2(h_\perp + \cos q)}{\varepsilon_q}\right) \in (-\pi, \pi]$ is the Bogoliubov angle. Writing the vacuum states in terms of the Bogoliubov modes yields

$$|0\rangle_{\text{NS/R}} = \prod_{0 < q \in \text{NS/R}} [\cos(\theta_q/2)]^{-1} \prod_{q \in \text{NS/R}, q \neq \pi} d_q |0\rangle_c, \quad (\text{S3})$$

where $|0\rangle_c$ now denotes the vacuum state of the Jordan-Wigner fermions. Since the number of Bogoliubov modes in $|0\rangle_{\text{NS/R}}$ grows linearly with system size, the size of the matrix A grows at most quadratically when calculating overlaps/matrix elements with the TFIC eigenstates. Current algorithms can calculate Pfaffians in $\mathcal{O}((2n)^3)$ time [50], enabling us to set up the truncated Hamiltonian efficiently for system sizes up to $N \sim 100$ sites.

Evaluating the matrix elements of the longitudinal field operator $V = -h_\parallel \sum_{j=1}^N \sigma_j^x$ can be further simplified significantly. Since V is translation-invariant it does not mix different momentum sectors of the truncated subspace, enabling efficient calculations through parallelization. Translation invariance further implies that only the matrix element of the longitudinal field at the first site needs to be evaluated, yielding the following formula:

$$\langle \phi_{k,\alpha} | V | \phi_{k,\beta} \rangle = -N h_\parallel \langle \phi_{k,\alpha} | (c_1^\dagger + c_1) | \phi_{k,\beta} \rangle. \quad (\text{S4})$$

Note also that because $\sigma_1^x = c_1^\dagger + c_1$ changes fermion parity, the above matrix element is non-vanishing only when $|\phi_{k,\alpha}\rangle$ and $|\phi_{k,\beta}\rangle$ have different fermion parity (i.e., one belongs to the NS sector and the other belongs to the R sector).